

# Aqueous Solution-Deposited Gallium Oxide Dielectric for Low-Temperature, Low-Operating-Voltage Indium Oxide Thin-Film Transistors: A Facile Route to Green Oxide Electronics

Wangying Xu,<sup>†</sup> Hongtao Cao,<sup>‡</sup> Lingyan Liang,<sup>‡</sup> and Jian-Bin Xu<sup>\*,†</sup>

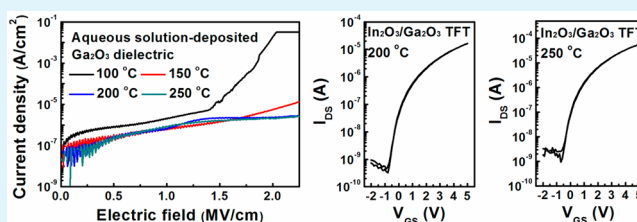
<sup>†</sup>Department of Electronic Engineering, Materials Science and Technology Research Center, The Chinese University of Hong Kong, Shatin, New Territories, Hong Kong, China

<sup>‡</sup>Division of Functional Materials and Nano Devices, Ningbo Institute of Materials Technology & Engineering, Chinese Academy of Sciences, Ningbo, China

## S Supporting Information

**ABSTRACT:** We reported a novel aqueous route to fabricate Ga<sub>2</sub>O<sub>3</sub> dielectric at low temperature. The formation and properties of Ga<sub>2</sub>O<sub>3</sub> were investigated by a wide range of characterization techniques, revealing that Ga<sub>2</sub>O<sub>3</sub> films could effectively block leakage current even after annealing in air at 200 °C. Furthermore, all aqueous solution-processed In<sub>2</sub>O<sub>3</sub>/Ga<sub>2</sub>O<sub>3</sub> TFTs fabricated at 200 and 250 °C showed mobilities of 1.0 and 4.1 cm<sup>2</sup> V<sup>-1</sup> s<sup>-1</sup>, on/off current ratio of ~10<sup>5</sup>, low operating voltages of 4 V, and negligible hysteresis. Our study represents a significant step toward the development of low-cost, low-temperature, and large-area green oxide electronics.

**KEYWORDS:** aqueous route, gallium oxide dielectric, indium oxide, oxide thin-film transistors, low-temperature, green oxide electronics



## 1. INTRODUCTION

Metal oxide semiconductors have attracted considerable attention as the channel materials for thin-film transistors (TFTs) due to their high carrier mobility and excellent uniformity.<sup>1–4</sup> Besides, the solution processability has opened new venues for low-cost and large-area oxide electronics.<sup>5–10</sup> Unfortunately, the sol–gel condensation, densification, and impurity removal typically require a high-temperature annealing step, which is one major obstacle in the fabrication of devices using flexible substrates.

Many attempts have been made to reduce the annealing temperature, and recent significant advances include sol–gel on a chip,<sup>8</sup> combustion process,<sup>9</sup> and deep-ultraviolet photochemical activation.<sup>10</sup> However, the use of toxic organic solvents such as 2-methoxyethanol (2-ME) in the majority of the reported studies would cause health risks and environmental impact. The environmentally friendly trend must also be seriously considered in future research. Most recently, some groups have demonstrated the aqueous precursor solution-processed indium oxide (In<sub>2</sub>O<sub>3</sub>) TFTs with good performance.<sup>11–13</sup> In this method, commercially available nitrate precursors are dissolved in water, which are then converted to the fully coordinated oxide during low annealing temperature. Because water is used as a solvent, the novel “aqueous route” is considered to be healthier, safer, and more environmentally friendly.

On the other hand, solution-processed oxide TFTs usually exhibited high operating voltages due to the use of thermally grown or vacuum-deposited SiO<sub>2</sub> as dielectrics. For this reason,

much effort has been devoted to develop novel gate dielectrics for low-power applications.<sup>14–26</sup> Among them, gallium oxide (Ga<sub>2</sub>O<sub>3</sub>) is one of the most promising dielectric materials due to its wide bandgap and good chemical/thermal stability.<sup>27–35</sup> However, most of the Ga<sub>2</sub>O<sub>3</sub> thin films were prepared by vacuum-based techniques such as sputter deposition,<sup>30,31,33</sup> electron beam evaporation,<sup>28</sup> chemical vapor deposition (CVD),<sup>27</sup> and atomic layer deposition (ALD),<sup>32</sup> which are not good for low-cost and large-scale fabrications. With the consideration that the group 13 ions of In(III) and Ga(III) exhibit similar chemical behavior in aqueous solution,<sup>36–39</sup> this raises the intriguing question of whether the aqueous route could be applied to fabricate Ga<sub>2</sub>O<sub>3</sub> dielectric and realize green oxide TFTs.

In this work, we developed a simple and low-temperature aqueous route to fabricate Ga<sub>2</sub>O<sub>3</sub> dielectric. The formation and properties of Ga<sub>2</sub>O<sub>3</sub> were investigated by a wide range of complementary characterization techniques. This method enables deposition of high-quality Ga<sub>2</sub>O<sub>3</sub> insulator at temperature as low as 200 °C. To evaluate Ga<sub>2</sub>O<sub>3</sub> as gate dielectrics, aqueous solution-processed In<sub>2</sub>O<sub>3</sub>/Ga<sub>2</sub>O<sub>3</sub> TFTs were fabricated with maximum annealing temperature of 200 and 250 °C, with resulting mobilities of 1.0 and 4.1 cm<sup>2</sup> V<sup>-1</sup> s<sup>-1</sup>, respectively. Besides, the devices showed low operating voltages of 4 V and negligible hysteresis.

Received: March 19, 2015

Accepted: June 9, 2015

Published: June 9, 2015

**Table 1.** Microstructural and Dielectric Properties of Ga<sub>2</sub>O<sub>3</sub> under Various Annealing Temperatures

| annealing temp (°C) | thickness (nm) | roughness (nm) | refractive index at 550 nm | leakage current at 2 MV/cm (A/cm <sup>2</sup> ) | capacitance (nF/cm <sup>2</sup> ) at 100 Hz | dielectric constant at 100 Hz |
|---------------------|----------------|----------------|----------------------------|---|---|-------------------------------|
| 100                 | 82             | 1.73           | 1.607                      | $1.8 \times 10^{-2}$                            | 151   | 14.0                          |
| 150                 | 65             | 0.84           | 1.653                      | $5.6 \times 10^{-6}$                            | 216   | 15.9                          |
| 200                 | 55             | 0.22           | 1.695                      | $2.4 \times 10^{-6}$                            | 193   | 12.2                          |
| 250                 | 52             | 0.19           | 1.719                      | $2.0 \times 10^{-6}$                            | 172   | 10.1                          |

## 2. EXPERIMENTAL SECTION

**2.1. Precursor Preparation.** All chemicals were purchased from Sigma-Aldrich and used as received without further purification. The Ga<sub>2</sub>O<sub>3</sub> precursor solution was prepared by dissolving gallium nitrate hydrate (Ga(NO<sub>3</sub>)<sub>3</sub>·xH<sub>2</sub>O) in water with a concentration of 1.0 M. The In<sub>2</sub>O<sub>3</sub> precursor solution was prepared by dissolving indium nitrate hydrate (In(NO<sub>3</sub>)<sub>3</sub>·xH<sub>2</sub>O) in water with a concentration of 0.15 M. Prior to spin coating, all the precursor solutions were ultrasonicated vigorously and then filtered through a 0.45 μm poly(ether sulfone) (PES) syringe.

**2.2. Film and Device Fabrication.** The heavily doped Si substrates were sonicated with acetone, isopropanol, and deionized water, respectively. The synthesized Ga<sub>2</sub>O<sub>3</sub> precursor solution was spin-coated at 3000 rpm for 20 s on substrates that were treated by oxygen plasma, and the coated layer was annealed at various temperatures (100, 150, 200, and 250 °C) for 0.5 h under ambient atmosphere. The spin coating and heat treatment processes were repeated again. For the metal–insulator–metal (MIM) devices, an Al electrode (100 nm) was deposited on the insulator layer by thermal evaporation. The area of the circular Al electrode was 0.03 mm<sup>2</sup>. Bottom-gate top-contact TFTs were fabricated by spin coating the In<sub>2</sub>O<sub>3</sub> solution on the annealed Ga<sub>2</sub>O<sub>3</sub> dielectric at 3000 rpm for 20 s and then annealed at desired temperatures for 1 h to achieve thicknesses of about 10 nm. Subsequently, the Al source and drain electrodes were deposited by thermal evaporation through a shadow mask. The channel width (*W*) and length (*L*) were 1500 and 100 μm, respectively. It has been shown that a small *W/L* ratio of 5 could induce mobility overestimation up to ~200% and the overestimation dropped to 10% as the *W/L* ratio increased to 10.<sup>15,21</sup> Therefore, the large *W/L* ratio over 15 in this study could efficiently limit mobility overestimation.

**2.3. Film and Device Characterization.** The thermal behavior of the Ga<sub>2</sub>O<sub>3</sub> precursor powder (dried at 110 °C for 12 h) was obtained by thermogravimetric analyzer (PerkinElmer, TGA 6) and differential scanning calorimeter (PerkinElmer, DSC 7) at a heating rate of 10 °C/min from 50 to 550 °C. The chemical characteristics of the Ga<sub>2</sub>O<sub>3</sub> films were examined by attenuated total reflectance Fourier transform infrared spectroscopy (ATR-FTIR, Bruker). The thicknesses and optical properties were measured via variable angle spectroscopic ellipsometry (J. A. Woollam Co., Inc.). The surface morphologies were characterized by atomic force microscopy (AFM, Veeco Dimension V). The structures were determined using X-ray diffraction (XRD, Siemens) with Cu Kα radiation. The frequency-dependent capacitance characteristics of the Ga<sub>2</sub>O<sub>3</sub> dielectrics were performed using a HP 4284A in a frequency range from 100 Hz to 1 MHz. The leakage of the Ga<sub>2</sub>O<sub>3</sub> films and the electrical characteristics of the TFTs were measured with a precision semiconductor analyzer (Keithley 4200) under ambient conditions. Threshold voltage (*V*<sub>th</sub>) was extracted from measurements in the saturation region by plotting (*I*<sub>DS</sub>)<sup>1/2</sup> versus *V*<sub>GS</sub> and extrapolating to *I*<sub>DS</sub> = 0 plots. The mobility (*μ*) and subthreshold swing (*S*) were calculated by the following formulas

$$I_{DS} = \left( \frac{\mu C_i W}{2L} \right) (V_{GS} - V_{th})^2$$

$$S = \left( \frac{d(\log_{10} I_{DS})}{dV_{GS}} \right)^{-1}$$

where *C<sub>i</sub>*, *W*, and *L* are the capacitance of the gate dielectrics per unit area, channel width, and channel length.

## 3. RESULTS AND DISCUSSION

To understand the conversion process from liquid precursor to solid Ga<sub>2</sub>O<sub>3</sub> film, systematical investigations with TG-DSC, ATR-FTIR, spectroscopic ellipsometry, XRD, and AFM characterization were carried out, and relevant results are summarized in Table 1. TGA-DSC measurement was initially performed as shown in Figure 1a. In general, the hydrolysis

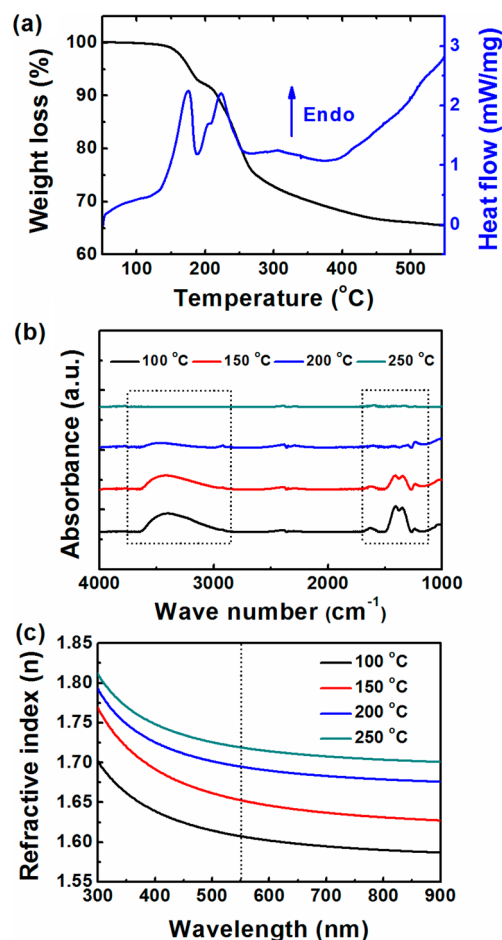


**Figure 1.** (a) TGA and DSC curves of Ga<sub>2</sub>O<sub>3</sub> powder from 50 to 550 °C. (b) ATR-FTIR spectra and (c) refractive index-wavelength curves of Ga<sub>2</sub>O<sub>3</sub> films annealed at indicated temperatures.

reaction took place in the range 100–150 °C.<sup>11–13,36–39</sup> However, no hydrolysis-related peaks were observed since the Ga<sub>2</sub>O<sub>3</sub> powder prepared at 110 °C was already hydrolyzed. The first endothermic peak at 174 °C indicates the dehydroxylation behavior of the hydrolyzed gallium hydroxide and forms metal oxide lattice.<sup>11–13</sup> Another peak at 224 °C could be related to the decomposition of residual nitrate.<sup>11–13</sup>

To further clarify the formation process of the Ga<sub>2</sub>O<sub>3</sub> thin film, ATR-FTIR measurements were performed, as shown in Figure 1b. The broad peak in the range 3000–3700 cm<sup>-1</sup>

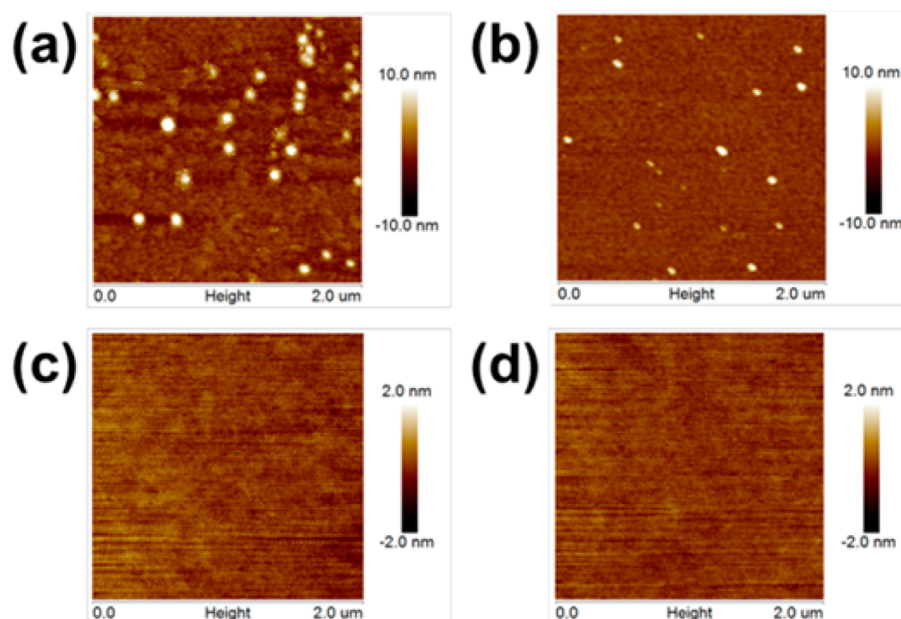


**Figure 2.** AFM images of Ga<sub>2</sub>O<sub>3</sub> films with different annealing temperatures of (a) 100, (b) 150, (c) 200, and (d) 250 °C. Images are 2 μm × 2 μm.

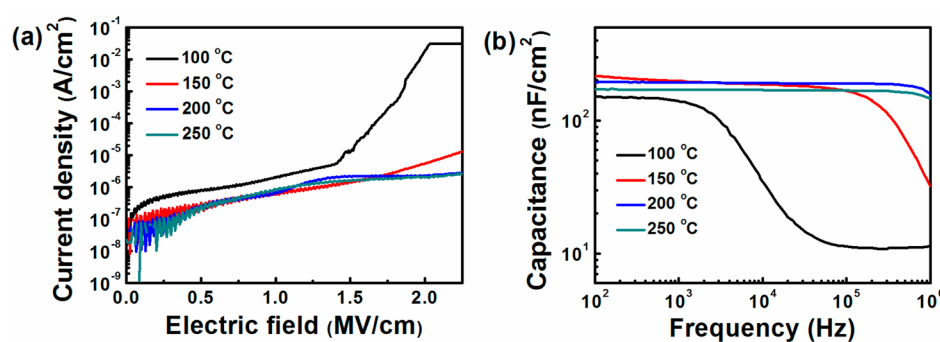


**Figure 3.** (a) Leakage current density vs electric field and (b) capacitance vs frequency of solution-processed Ga<sub>2</sub>O<sub>3</sub> dielectrics annealed at indicated temperatures.

corresponds to hydroxyl (OH) group stretching vibrations.<sup>12,13</sup> The peak in the 1200–1700 cm<sup>-1</sup> range could be assigned to hydroxyl group or nitrate (NO<sub>3</sub><sup>-</sup>) deformation vibrations.<sup>12,13,20,21</sup> The 100 °C annealed film contained a large amount of hydroxyl and nitrate groups. As the annealing temperature increased, the hydroxyl and nitrate groups were gradually decomposed and completely removed at 250 °C.

To verify the condensation and densification behavior of the Ga<sub>2</sub>O<sub>3</sub> film, spectroscopic ellipsometry measurements were performed. The thickness of the Ga<sub>2</sub>O<sub>3</sub> decreased from 82 to 52 nm as the annealing temperature increased from 100 to 250 °C, which is due to the evaporation of solvent and the densification process of the thin film. Figure 1c shows the refractive index–wavelength curves of Ga<sub>2</sub>O<sub>3</sub> films annealed under various temperatures. Note that the refractive index is the indicator of the packing density of the thin films.<sup>22,31</sup> The increase of the refractive index with the rise of annealing temperature could be attributed to the evaporation of solvent and decomposition of the nitrate and hydroxyl groups, in agreement with the reduction of thickness. The film annealed at 250 °C showed refractive index of 1.719 at 550 nm, which is comparable to the low-temperature vacuum-deposited counterpart.<sup>24,31,32</sup> Besides, the optical bandgaps of the Ga<sub>2</sub>O<sub>3</sub> films determined from the spectroscopic ellipsometry were in the

range 5.46–5.64 eV (Supporting Information Figure S1), similar to the reported values.<sup>31,32</sup> The wide bandgap of the dielectric material is good for restricting the leakage current.

Figure S2 in the Supporting Information shows the XRD spectra of Ga<sub>2</sub>O<sub>3</sub> films as a function of annealing temperature. The Ga<sub>2</sub>O<sub>3</sub> films showed an amorphous phase up to 250 °C. Previous studies have demonstrated that the Ga<sub>2</sub>O<sub>3</sub> could maintain amorphous state up to 500 °C.<sup>31,33</sup> The amorphous structure is desirable because grain boundaries usually act as preferential paths for impurity diffusion and leak current.<sup>16</sup> Figure 2 shows the AFM images of Ga<sub>2</sub>O<sub>3</sub> thin films treated at different temperatures. The root-mean-square (rms) roughness of Ga<sub>2</sub>O<sub>3</sub> films annealed at 100, 150, 200, and 250 °C were 1.73, 0.84, 0.22, and 0.19 nm, respectively. Note that there were considerable quantities of gaseous byproducts such as H<sub>2</sub>O and N<sub>2</sub> evolved in the conversion process. These gaseous byproducts could not be easily removed at low temperature, making the film discontinuous and rough.<sup>9</sup> The Ga<sub>2</sub>O<sub>3</sub> film showed ultrasmooth surface as the annealing temperature rose up to 200 °C, consistent with the amorphous structure, which is ideal for suppressing the surface roughness induced leakage current and achieving high charge carrier mobility in the TFT channel.<sup>14,16</sup> From the above TGA-DSC, ATR-FTIR, spectroscopic ellipsometry, XRD, and AFM results, we could conclude

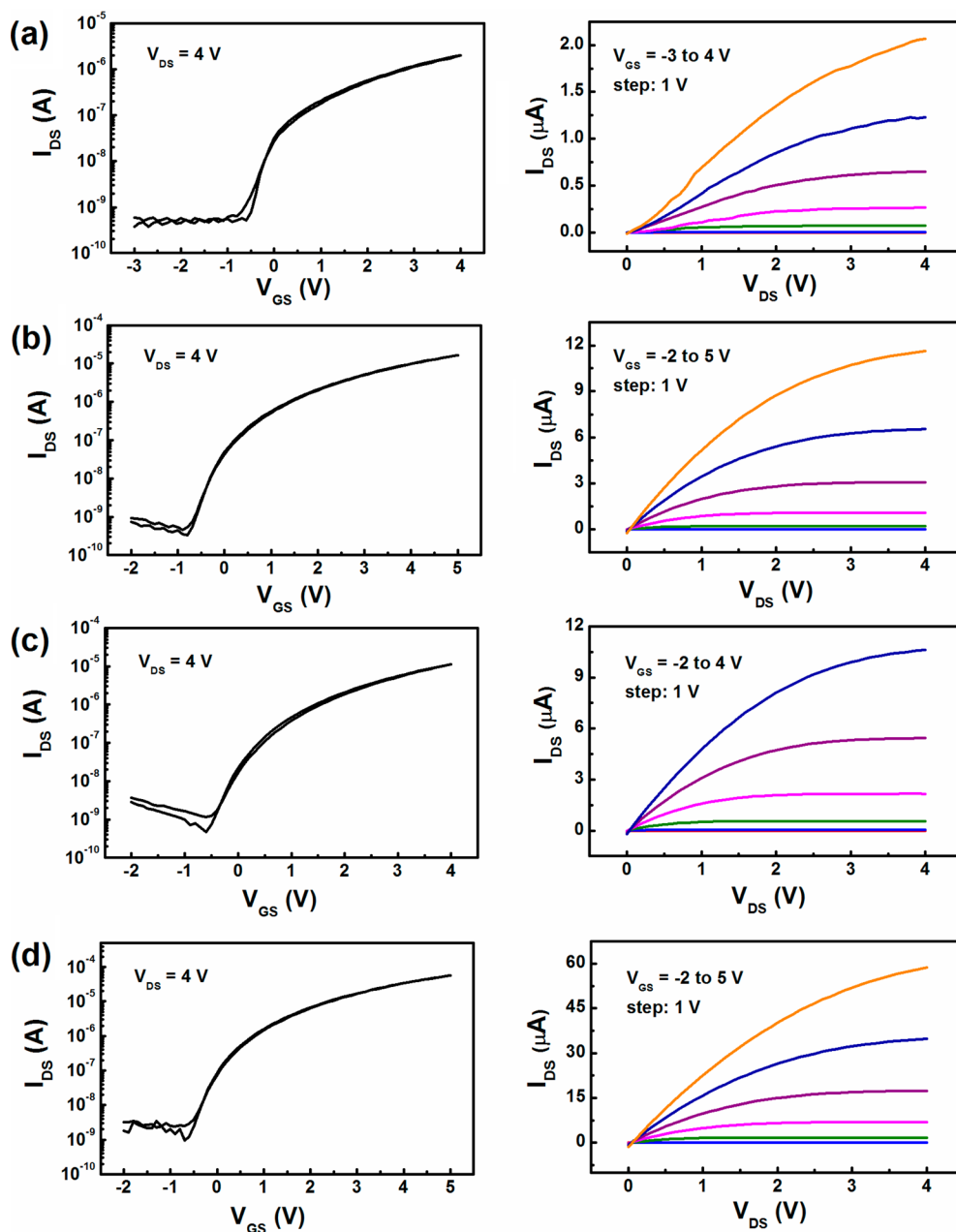


**Figure 4.** Transfer and output characteristics of (a)  $\text{In}_2\text{O}_3$  (185 °C)/ $\text{Ga}_2\text{O}_3$  (200 °C) TFT, (b)  $\text{In}_2\text{O}_3$  (200 °C)/ $\text{Ga}_2\text{O}_3$  (200 °C) TFT, (c)  $\text{In}_2\text{O}_3$  (200 °C)/ $\text{Ga}_2\text{O}_3$  (250 °C) TFT, and (d)  $\text{In}_2\text{O}_3$  (250 °C)/ $\text{Ga}_2\text{O}_3$  (250 °C) TFT.

that the aqueous-derived  $\text{Ga}_2\text{O}_3$  film undergoes the decomposition of the nitrate and hydroxyl groups, as well as the formation of metal oxide framework after low-temperature post-annealing treatment.

The dielectric properties of  $\text{Ga}_2\text{O}_3$  were measured by MIM structures and summarized in Table 1. As shown in Figure 3a, the 100 °C annealed device showed large leakage current due to the existence of large amounts of nitrate and hydroxyl groups. The 200 °C and 250 °C annealed films showed low leakage currents of  $2.4 \times 10^{-6}$  A/cm<sup>2</sup> and  $2.0 \times 10^{-6}$  A/cm<sup>2</sup> at 2 MV/cm, which were attributed to the decomposition of hydroxyl and nitrate groups as well as the formation of metal oxide framework.<sup>19–21</sup> The capacitance–frequency curves in the range 100 Hz to 1 MHz are shown in Figure 3b. The films annealed at 200 and 250 °C had capacitances of 193 and 172 nF/cm<sup>2</sup>, corresponding to dielectric constants of 12.2 and 10.1,

similar to the reported vacuum-fabricated counterparts.<sup>27,32</sup> The weak frequency dependence of capacitance at high annealing temperature is consistent with the low leakage current of insulator, suggesting low defect concentrations.<sup>3,16</sup> The dielectric properties of  $\text{Ga}_2\text{O}_3$  are in good agreement with the above thin-film characterization.

To demonstrate the feasibility of using  $\text{Ga}_2\text{O}_3$  as gate dielectrics, we fabricated bottom-gate top-contact TFTs employing previous reported aqueous-derived  $\text{In}_2\text{O}_3$  as channel layer.<sup>11–13</sup> Figure 4 demonstrates the transfer and output characteristics of  $\text{In}_2\text{O}_3/\text{Ga}_2\text{O}_3$  TFTs under various annealing temperatures, with electrical performance summarized in Table 2. The  $\text{In}_2\text{O}_3$  (185 °C)/ $\text{Ga}_2\text{O}_3$  (200 °C) TFT showed a low mobility of  $0.2 \text{ cm}^2 \text{ V}^{-1} \text{ s}^{-1}$  (Figure 4a), whereas the  $\text{In}_2\text{O}_3$  (200 °C)/ $\text{Ga}_2\text{O}_3$  (200 °C) TFT exhibited an acceptable mobility of  $1.0 \text{ cm}^2 \text{ V}^{-1} \text{ s}^{-1}$ , subthreshold swing  $0.28 \text{ V/decade}$ ,

**Table 2. Electrical Performance of In<sub>2</sub>O<sub>3</sub>/Ga<sub>2</sub>O<sub>3</sub> TFTs under Various Annealing Temperatures**

| TFTs  | mobility (cm <sup>2</sup> V <sup>-1</sup> s <sup>-1</sup> ) | subthreshold swing (V/decade) | threshold voltage (V) | on/off current ratio |
|---|---|-------------------------------|-----------------------|----------------------|
| In <sub>2</sub> O <sub>3</sub> (185 °C)/Ga <sub>2</sub> O <sub>3</sub> (200 °C) | 0.2 ± 0.1   | 0.26 ± 0.04                   | 0.4 ± 0.4             | ~10 <sup>4</sup>     |
| In <sub>2</sub> O <sub>3</sub> (200 °C)/Ga <sub>2</sub> O <sub>3</sub> (200 °C) | 1.0 ± 0.3   | 0.28 ± 0.03                   | 0.6 ± 0.2             | ~10 <sup>5</sup>     |
| In <sub>2</sub> O <sub>3</sub> (200 °C)/Ga <sub>2</sub> O <sub>3</sub> (250 °C) | 1.0 ± 0.2   | 0.29 ± 0.04                   | 0.7 ± 0.3             | ~10 <sup>5</sup>     |
| In <sub>2</sub> O <sub>3</sub> (250 °C)/Ga <sub>2</sub> O <sub>3</sub> (250 °C) | 4.1 ± 0.6   | 0.26 ± 0.04                   | 0.6 ± 0.3             | ~10 <sup>5</sup>     |

threshold voltage of 0.6 V, and on/off current ratio of ~10<sup>5</sup> (Figure 4b). The In<sub>2</sub>O<sub>3</sub> (200 °C)/Ga<sub>2</sub>O<sub>3</sub> (250 °C) TFT (Figure 4c) showed similar performance to the In<sub>2</sub>O<sub>3</sub> (200 °C)/Ga<sub>2</sub>O<sub>3</sub> (200 °C) one. A remarkable improvement was observed for the In<sub>2</sub>O<sub>3</sub> (250 °C)/Ga<sub>2</sub>O<sub>3</sub> (250 °C) TFT (Figure 4d), exhibiting a good mobility of 4.1 cm<sup>2</sup> V<sup>-1</sup> s<sup>-1</sup>, subthreshold swing 0.26 V/decade, threshold voltage of 0.6 V, and on/off current ratio of ~10<sup>5</sup>. According to the above results, the device performance (mobility) is mainly dependent on the annealing temperature of the In<sub>2</sub>O<sub>3</sub> semiconductor. The device showed improved performance as the annealing temperature of In<sub>2</sub>O<sub>3</sub> increased from 185 to 250 °C. This is consistent with the previous studies on aqueous-derived In<sub>2</sub>O<sub>3</sub> TFTs using thermally SiO<sub>2</sub> or solution-processed ZrO<sub>2</sub> dielectrics and could be attributed to the formation of indium oxide framework as well as the decomposition of nitrate and hydroxyl groups with the rise of annealing temperature.<sup>11–13</sup> Besides, the In<sub>2</sub>O<sub>3</sub>/Ga<sub>2</sub>O<sub>3</sub> TFTs exhibited low operating voltages of 4 V and negligible hysteresis. These impressive results achieved by a simple and green process are comparable to the recently reported low-temperature solution-processed high-*k* dielectric/oxide semiconductor TFTs.<sup>12,13,19,23–26</sup> Besides, we have carried out the positive and negative bias stress study of In<sub>2</sub>O<sub>3</sub>/Ga<sub>2</sub>O<sub>3</sub> TFTs at maximum processed temperature of 200 and 250 °C, as shown in Supporting Information Figure S3. The 250 °C annealed device showed better bias stress stability, owing to the improvement of In<sub>2</sub>O<sub>3</sub> semiconductor quality and semiconductor/dielectric interface; detailed analysis can be found in the Supporting Information.

The use of water as solvent plays an important role in achieving respectably performing In<sub>2</sub>O<sub>3</sub>/Ga<sub>2</sub>O<sub>3</sub> TFTs at low temperature. First, water is an excellent solvent because it has no organic residues to be removed for obtaining high-quality films.<sup>11–13</sup> Second, the large dielectric constant of water (>80) could effectively weaken the electrostatic force between the cation (In<sup>3+</sup> or Ga<sup>3+</sup>) and anion (NO<sub>3</sub><sup>-</sup>). In aqueous solutions, In<sup>3+</sup> or Ga<sup>3+</sup> usually exists in the form of outer-sphere complex [In(OH<sub>2</sub>)<sub>6</sub><sup>3+</sup>NO<sub>3</sub><sup>-</sup>]/[Ga(OH<sub>2</sub>)<sub>6</sub><sup>3+</sup>NO<sub>3</sub><sup>-</sup>] and/or [In(OH<sub>2</sub>)<sub>6</sub><sup>3+</sup>]/[Ga(OH<sub>2</sub>)<sub>6</sub><sup>3+</sup>] with free nitrate.<sup>11–13,36–39</sup> As the coordination bond between the cation and neighboring aquo ion is relatively weak, it is easily broken with low thermal energy.<sup>11–13</sup> Thus, dense and smooth films could be achieved at low annealing temperatures. Further improvement of the device performance could be achieved by optimization of the channel layer, dielectric layer, channel/dielectric interface, as well as the introduction of passivation layer.

## 4. CONCLUSION

In summary, we have demonstrated the low-temperature fabrication of high-quality Ga<sub>2</sub>O<sub>3</sub> dielectric via an aqueous solution process. The thin-film formation and properties of Ga<sub>2</sub>O<sub>3</sub> were investigated by various characterization techniques including TGA-DSC, ATR-FTIR, spectroscopic ellipsometry, XRD, AFM, and electrical measurements. Besides, aqueous solution-deposited In<sub>2</sub>O<sub>3</sub>/Ga<sub>2</sub>O<sub>3</sub> TFTs fabricated at 200 and 250 °C exhibited good mobilities of 1.0 and 4.1 cm<sup>2</sup> V<sup>-1</sup> s<sup>-1</sup>, as well as on/off current ratio of ~10<sup>5</sup>. Our finding provides potential for realizing low-cost, low-temperature, and large-area green oxide electronics.

## ■ ASSOCIATED CONTENT

### Supporting Information

Optical bandgap of the Ga<sub>2</sub>O<sub>3</sub>, XRD spectra of Ga<sub>2</sub>O<sub>3</sub>, and bias stress stability of In<sub>2</sub>O<sub>3</sub>/Ga<sub>2</sub>O<sub>3</sub> TFTs. The Supporting Information is available free of charge on the ACS Publications website at DOI: 10.1021/acsami.5b02451.

## ■ AUTHOR INFORMATION

### Corresponding Author

\*E-mail: jbxu@ee.cuhk.edu.hk.

### Notes

The authors declare no competing financial interest.

## ■ ACKNOWLEDGMENTS

The work was in part supported by the Research Grants Council of Hong Kong, particularly via Grants AoE/P-03/08, N\_CUHK405/12, and CUHK Group Research Scheme. J.-B.X. would like to thank the National Science Foundation of China for the support, particularly via Grant 61229401.

## ■ REFERENCES

- (1) Fortunato, E.; Barquinha, P.; Martins, R. Oxide Semiconductor Thin-Film Transistors: A Review of Recent Advances. *Adv. Mater.* **2012**, *24*, 2945–2986.
- (2) Nomura, K.; Ohta, H.; Takagi, A.; Kamiya, T.; Hirano, M.; Hosono, H. Room-Temperature Fabrication of Transparent Flexible Thin-Film Transistors Using Amorphous Oxide Semiconductors. *Nature* **2004**, *432*, 488–492.
- (3) Xu, W.; Dai, M.; Liang, L.; Liu, Z.; Sun, X.; Wan, Q.; Cao, H. Anomalous Bias-Stress-Induced Unstable Phenomena of InZnO Thin-Film Transistors Using Ta<sub>2</sub>O<sub>5</sub> Gate Dielectric. *J. Phys. D: Appl. Phys.* **2012**, *45*, 205103.
- (4) Park, J. S.; Maeng, W.-J.; Kim, H.-S.; Park, J.-S. Review of Recent Developments in Amorphous Oxide Semiconductor Thin-Film Transistor Devices. *Thin Solid Films* **2012**, *520*, 1679–1693.
- (5) Jeong, S.; Moon, J. Low-Temperature, Solution-Processed Metal Oxide Thin Film Transistors. *J. Mater. Chem.* **2012**, *22*, 1243–1250.
- (6) Xu, W.; Liu, D.; Wang, H.; Ye, L.; Miao, Q.; Xu, J.-B. Facile Passivation of Solution-Processed InZnO Thin-Film Transistors by Octadecylphosphonic Acid Self-Assembled Monolayers at Room Temperature. *Appl. Phys. Lett.* **2014**, *104*, 173504.
- (7) Thomas, S. R.; Pattanasattayavong, P.; Anthopoulos, T. D. Solution-Processable Metal Oxide Semiconductors for Thin-Film Transistor Applications. *Chem. Soc. Rev.* **2013**, *42*, 6910–6923.
- (8) Banger, K. K.; Yamashita, Y.; Mori, K.; Peterson, R. L.; Leedham, T.; Rickard, J.; Sirringhaus, H. Low-Temperature, High-Performance Solution-Processed Metal Oxide Thin-Film Transistors Formed by a “Sol–Gel on Chip” Process. *Nat. Mater.* **2011**, *10*, 45–50.
- (9) Kim, M. G.; Kanatzidis, M. G.; Facchetti, A.; Marks, T. J. Low-Temperature Fabrication of High-Performance Metal Oxide Thin-Film Electronics Via Combustion Processing. *Nat. Mater.* **2011**, *10*, 382–388.

- (10) Kim, Y. H.; Heo, J. S.; Kim, T. H.; Park, S.; Yoon, M. H.; Kim, J.; Oh, M. S.; Yi, G. R.; Noh, Y. Y.; Park, S. K. Flexible Metal-Oxide Devices Made by Room-Temperature Photochemical Activation of Sol-Gel Films. *Nature* **2012**, *489*, 128–U191.
- (11) Hwang, Y. H.; Seo, J.-S.; Yun, J. M.; Park, H.; Yang, S.; Park, S.-H. K.; Bae, B.-S. An “Aqueous Route” for the Fabrication of Low-Temperature-Processable Oxide Flexible Transparent Thin-Film Transistors on Plastic Substrates. *NPG Asia Mater.* **2013**, *5*, e45.
- (12) Park, J. H.; Yoo, Y. B.; Lee, K. H.; Jang, W. S.; Oh, J. Y.; Chae, S. S.; Lee, H. W.; Han, S. W.; Baik, H. K. Boron-Doped Peroxo-Zirconium Oxide Dielectric for High-Performance, Low-Temperature, Solution-Processed Indium Oxide Thin-Film Transistor. *ACS Appl. Mater. Interfaces* **2013**, *5*, 8067–8075.
- (13) Liu, A.; Liu, G. X.; Zhu, H. H.; Xu, F.; Fortunato, E.; Martins, R.; Shan, F. K. Fully Solution-Processed Low-Voltage Aqueous In<sub>2</sub>O<sub>3</sub> Thin-Film Transistors Using an Ultrathin ZrO<sub>x</sub> Dielectric. *ACS Appl. Mater. Interfaces* **2014**, *6*, 17364–17369.
- (14) Avis, C.; Jang, J. High-Performance Solution Processed Oxide TFT with Aluminum Oxide Gate Dielectric Fabricated by a Sol-Gel Method. *J. Mater. Chem.* **2011**, *21*, 10649–10652.
- (15) Huang, G.; Duan, L.; Dong, G.; Zhang, D.; Qiu, Y. High-Mobility Solution-Processed Tin Oxide Thin-Film Transistors with High- $\kappa$  Alumina Dielectric Working in Enhancement Mode. *ACS Appl. Mater. Interfaces* **2014**, *6*, 20786–20794.
- (16) Xu, W.; Wang, H.; Ye, L.; Xu, J. The Role of Solution-Processed High- $\kappa$  Gate Dielectrics in Electrical Performance of Oxide Thin-Film Transistors. *J. Mater. Chem. C* **2014**, *2*, 5389–5396.
- (17) Nayak, P. K.; Hedhili, M. N.; Cha, D.; Alshareef, H. N. High Performance In<sub>2</sub>O<sub>3</sub> Thin Film Transistors Using Chemically Derived Aluminum Oxide Dielectric. *Appl. Phys. Lett.* **2013**, *103*, 033518.
- (18) Park, J. H.; Yoo, Y. B.; Lee, K. H.; Jang, W. S.; Oh, J. Y.; Chae, S. S.; Baik, H. K. Low-Temperature, High-Performance Solution-Processed Thin-Film Transistors with Peroxo-Zirconium Oxide Dielectric. *ACS Appl. Mater. Interfaces* **2013**, *5*, 410–417.
- (19) Yang, W.; Song, K.; Jung, Y.; Jeong, S.; Moon, J. Solution-Deposited Zr-Doped AlO<sub>x</sub> Gate Dielectrics Enabling High-Performance Flexible Transparent Thin Film Transistors. *J. Mater. Chem. C* **2013**, *1*, 4275–4282.
- (20) Park, J. H.; Kim, K.; Yoo, Y. B.; Park, S. Y.; Lim, K.-H.; Lee, K. H.; Baik, H. K.; Kim, Y. S. Water Adsorption Effects of Nitrate Ion Coordinated Al<sub>2</sub>O<sub>3</sub> Dielectric for High Performance Metal-Oxide Thin-Film Transistor. *J. Mater. Chem. C* **2013**, *1*, 7166–7174.
- (21) Xu, W.; Wang, H.; Xie, F.; Chen, J.; Cao, H.; Xu, J.-B. Facile and Environmentally Friendly Solution-Processed Aluminum Oxide Dielectric for Low-Temperature, High-Performance Oxide Thin-Film Transistors. *ACS Appl. Mater. Interfaces* **2015**, *7*, 5803–5810.
- (22) Liang, L. Y.; Cao, H. T.; Liu, Q.; Jiang, K. M.; Liu, Z. M.; Zhuge, F.; Deng, F. L. Substrate Biasing Effect on the Physical Properties of Reactive Rf-Magnetron-Sputtered Aluminum Oxide Dielectric Films on ITO Glasses. *ACS Appl. Mater. Interfaces* **2014**, *6*, 2255–2261.
- (23) Yoo, Y. B.; Park, J. H.; Lee, K. H.; Lee, H. W.; Song, K. M.; Lee, S. J.; Baik, H. K. Solution-Processed High- $k$  HfO<sub>2</sub> Gate Dielectric Processed under Softening Temperature of Polymer Substrates. *J. Mater. Chem. C* **2013**, *1*, 1651–1658.
- (24) Xu, X. L.; Cui, Q. Y.; Jin, Y. Z.; Guo, X. J. Low-Voltage Zinc Oxide Thin-Film Transistors with Solution-Processed Channel and Dielectric Layers Below 150 °C. *Appl. Phys. Lett.* **2012**, *101*, 222114.
- (25) Bae, E. J.; Kang, Y. H.; Han, M.; Lee, C.; Cho, S. Y. Soluble Oxide Gate Dielectrics Prepared Using the Self-Combustion Reaction for High-Performance Thin-Film Transistors. *J. Mater. Chem. C* **2014**, *2*, 5695–5703.
- (26) Lin, Y.; Faber, H.; Zhao, K.; Wang, Q.; Amassian, A.; McLachlan, M.; Anthopoulos, T. D. High-Performance ZnO Transistors Processed Via an Aqueous Carbon-Free Metal Oxide Precursor Route at Temperatures Between 80–180 °C. *Adv. Mater.* **2013**, *25*, 4340–4346.
- (27) Pal, S.; Ray, S. K.; Chakraborty, B. R.; Lahiri, S. K.; Bose, D. N. Gd<sub>2</sub>O<sub>3</sub>, Ga<sub>2</sub>O<sub>3</sub> (Gd<sub>2</sub>O<sub>3</sub>), Y<sub>2</sub>O<sub>3</sub>, and Ga<sub>2</sub>O<sub>3</sub>, as High- $k$  Gate Dielectrics on SiGe: A Comparative Study. *J. Appl. Phys.* **2001**, *90*, 4103–4107.
- (28) Al-Kuhaili, M. F.; Durrani, S. M. A.; Khawaja, E. E. Optical Properties of Gallium Oxide Films Deposited by Electron-Beam Evaporation. *Appl. Phys. Lett.* **2003**, *83*, 4533–4535.
- (29) Chen, C. P.; Lee, Y. J.; Chang, Y. C.; Yang, Z. K.; Hong, M.; Kwo, J.; Lee, H. Y.; Lay, T. S. Structural and Electrical Characteristics of Ga<sub>2</sub>O<sub>3</sub>(Gd<sub>2</sub>O<sub>3</sub>)/GaAs under High Temperature Annealing. *J. Appl. Phys.* **2006**, *100*, 104502.
- (30) Marie, P.; Portier, X.; Cardin, J. Growth and Characterization of Gallium Oxide Thin Films by Radiofrequency Magnetron Sputtering. *Phys. Status Solidi A* **2008**, *205*, 1943–1946.
- (31) Ramana, C. V.; Rubio, E. J.; Barraza, C. D.; Miranda Gallardo, A.; McPeak, S.; Kotru, S.; Grant, J. T. Chemical Bonding, Optical Constants, and Electrical Resistivity of Sputter-Deposited Gallium Oxide Thin Films. *J. Appl. Phys.* **2014**, *115*, 043508.
- (32) Choi, D.-W.; Chung, K.-B.; Park, J.-S. Low Temperature Ga<sub>2</sub>O<sub>3</sub> Atomic Layer Deposition Using Gallium Tri-isopropoxide and Water. *Thin Solid Films* **2013**, *546*, 31–34.
- (33) Kumar, S. S.; Rubio, E. J.; Noor-A-Alam, M.; Martinez, G.; Manandhar, S.; Shutthanandan, V.; Thevuthasan, S.; Ramana, C. V. Structure, Morphology, and Optical Properties of Amorphous and Nanocrystalline Gallium Oxide Thin Films. *J. Phys. Chem. C* **2013**, *117*, 4194–4200.
- (34) Paterson, G. W.; Wilson, J. A.; Moran, D.; Hill, R.; Long, A. R.; Thayne, I.; Passlack, M.; Droopad, R. Gallium oxide (Ga<sub>2</sub>O<sub>3</sub>) on Gallium Arsenide—A Low Defect, High-K System for Future Devices. *Mater. Sci. Eng., B* **2006**, *135*, 277–281.
- (35) Chang, T. H.; Chiu, C. J.; Chang, S. J.; Tsai, T. Y.; Yang, T. H.; Huang, Z. D.; Weng, W. Y. Amorphous InGaZnO Ultraviolet Phototransistors with Double-Stack Ga<sub>2</sub>O<sub>3</sub>/SiO<sub>2</sub> Dielectric. *Appl. Phys. Lett.* **2013**, *10*, 221104.
- (36) Rudolph, W. W.; Pye, C. C. Gallium(III) Hydration in Aqueous Solution of Perchlorate, Nitrate and Sulfate. Raman and 71-Ga NMR Spectroscopic Studies and ab Initio Molecular Orbital Calculations of Gallium(III) Water Clusters. *Phys. Chem. Chem. Phys.* **2002**, *4*, 4319–4327.
- (37) Rudolph, W. W.; Pye, C. C.; Irmer, G. Study of Gallium(III) Nitrate Hydrate and Aqueous Solutions: Raman Spectroscopy and ab Initio Molecular Orbital Calculations of Gallium(III) Water Clusters. *J. Raman Spectrosc.* **2002**, *33*, 177–190.
- (38) Rudolph, W. W.; Fischer, D.; Tomney, M. R.; Pye, C. C. Indium(III) Hydration in Aqueous Solutions of Perchlorate, Nitrate and Sulfate. Raman and Infrared Spectroscopic Studies and ab-initio Molecular Orbital Calculations of Indium(III)-Water Clusters. *Phys. Chem. Chem. Phys.* **2004**, *6*, 5145–5155.
- (39) Harris, W. R.; Messori, L. A Comparative Study of Aluminum(III), Gallium(III), Indium(III), and Thallium(III) Binding to Human Serum Transferrin. *Coord. Chem. Rev.* **2002**, *228*, 237–262.